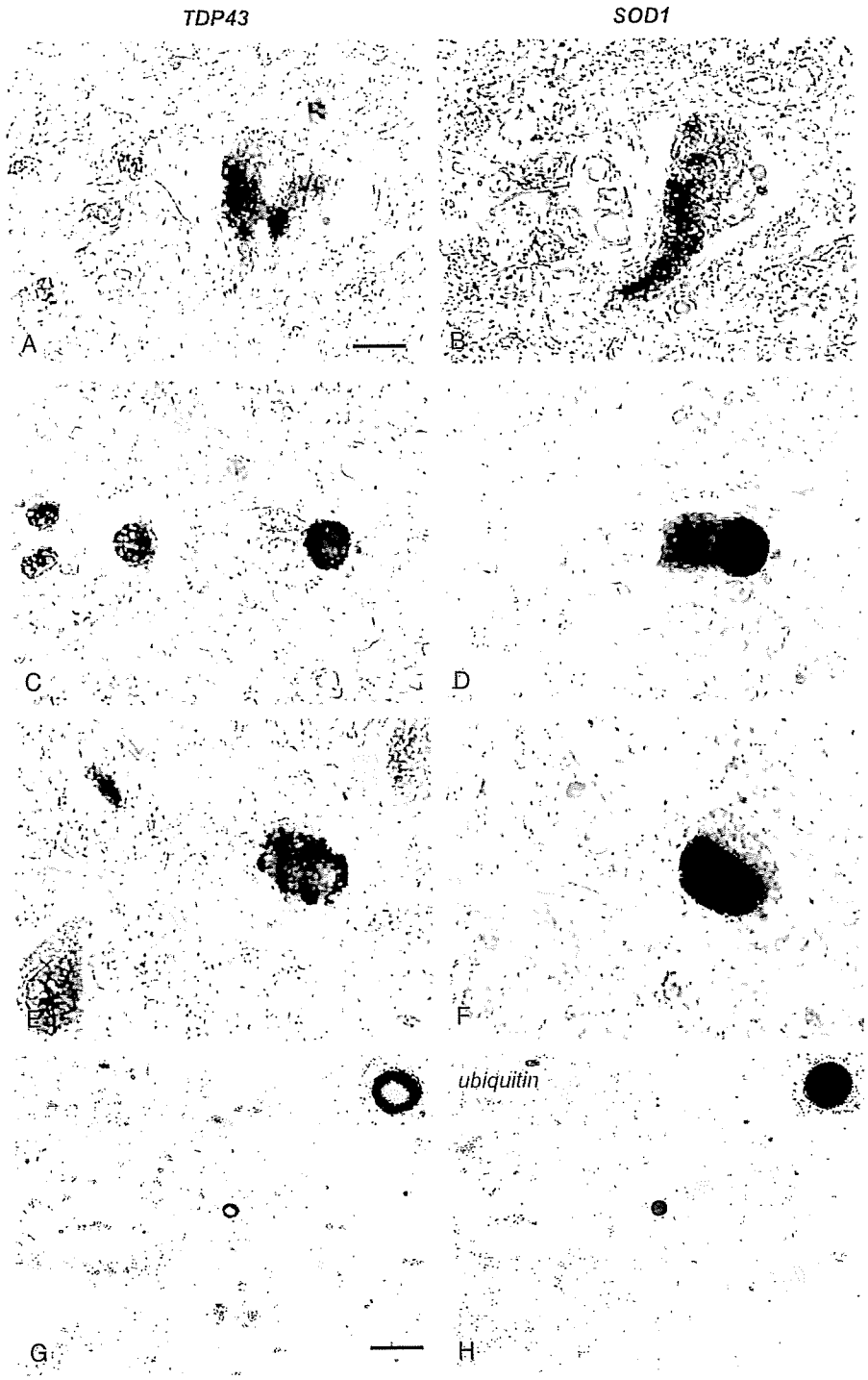

FIGURE 2. Colocalization of TAR DNA binding protein (TDP) and superoxide dismutase 1 (SOD1) in neurons of an amyotrophic lateral sclerosis 1 (C111Y) patient. **(A, B)** Heterogeneous cytoplasmic staining patterns for TDP **(A)** and for SOD1 **(B)**. The nucleus is TDP negative. **(C–F)** Neuronal inclusions are positive for TDP **(C, E)** and SOD1 **(D, F)**. **(G, H)** The halo portion of a Lewy body–like hyaline inclusion (LBHI) is stained strongly for TDP **(G)** and ubiquitin **(H)**. The upper panels are high-magnification views of each LBHI. Immunohistochemistry: **(A, C, E, G)** = TDP; **(B, D, F)** = SOD1; **(H)** = ubiquitin. **(B, D, F,** and **H)** are adjacent serial sections of **(A, C, E,** and **G)**, respectively. Scale bars = **(A–F)** 10 μm; **(G, H)** 50 μm; insets in **(G, H)** = 16 μm.

an aggregation pattern (Figs. 2A–F). The TDP and ubiquitin were also colocalized in inclusions (Figs. 2G, H). Patients ALS1-2 (30) and ALS1-3 (31) possessed the same SOD1 mutation; TDP-IR of the nuclei was weaker in Patient ALS1-3,who had more LBHIs than Patient ALS1-2. The TDP-IR of some of the LBHIs observed in these patients was weak, but stronger than that in most of the nuclei (Fig. 3A). Colocalization of TDP and SOD1 was demonstrated in LBHIs in serial sections (Figs. 3A, B). The LBHIs were scarce in other ALS1 patients. Although TDP-IR was retained in the nuclei of most of the residual neurons in Patients ALS1-4 (G37R) (32) and ALS1-5 (L126S) (33), there were a few neurons with TDP-negative nuclei and cytoplasm. The TDP-negative nuclei were atrophic or deformed (Fig. 3D), whereas most of the TDP-positive nuclei were circular (Fig. 3F). In ALS1 patients, there was no apparent relationship between nuclear TDP-IR and disease duration. The SMI31-positive conglomerate inclusions (Fig. 3E) in Patients ALS1-5 and ALS1-6 were mostly TDP negative (Fig. 3F) or had only very faint staining (Fig. 3D).

G93A Mice

In normal littermates, TDP-IR was found in the neurons and some glia in the gray matter (Fig. 4A); the white matter was negative for TDP. In G1L mice, the nuclei of neurons and reactive astrocytes were stained for TDP. The

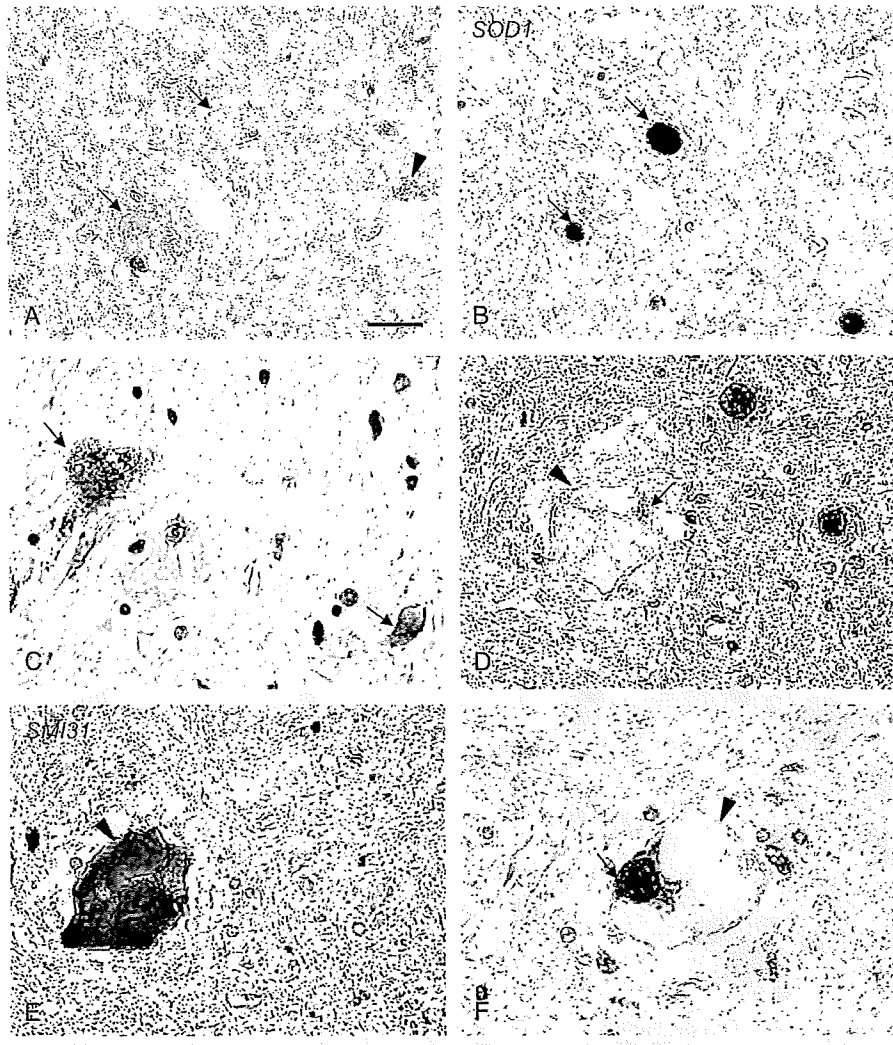

FIGURE 3. TAR DNA binding protein (TDP) staining patterns in the other amyotrophic lateral sclerosis 1 patients. **(A, B)** Superoxide dismutase 1 (SOD1)–positive Lewy body–like hyaline inclusions **(B)** are weakly stained (left, arrow) and very faintly stained (right, arrow) for TDP **(A)**. There is mislocalization in a small neuron (arrowhead) in **(A)**. **(C)** The neuron cytoplasm is diffusely stained for TDP (arrows). **(D, E)** A conglomerate inclusion is positive for SMI31 (**[E]** arrowhead) and is negative for TDP (**[D]** arrowhead). The nucleus (**[D]** arrow) is atrophic and deformed. **(F)** The TDP-positive nucleus (arrow) in a neuron containing a TDP-negative conglomerate inclusion (arrowhead) appears round and intact. Immunohistochemistry: **(A, C, D, F)** = TDP; **(B)** = SOD1; **(E)** = phosphorylated neurofilament (SMI31). **(B)** and **(E)** are serial sections of **(A)** and **(D)**, respectively. Scale bar = 20 μm.

cytoplasm of a few anterior horn cells showed a punctate TDP staining pattern, but most of the neuron nuclei were TDP positive (Figs. 4E, 5C). Neurons with TDP-negative nuclei and TDP-positive cytoplasm were rare (Fig. 4B). The TDP-positive inclusions and neurites were numerous (Figs. 4C, 5A–D), and the nuclear TDP-IR of these cells was weak (Fig. 5A). Some vacuoles were also stained for TDP (Fig. 4C). Colocalization of TDP and SOD1 was also detected in LBHIs in serial sections (Figs. 4C, D). Nuclear TDP-IR varied widely from mouse to mouse (Stages 1–4, Figs. 5A–D). In G1L mice showing a rapid clinical course and prominent LBHI-formation, nuclear TDP-IR was weak (Stage 1, Figs. 5A, E), whereas G1L mice showing a slow clinical course and less LBHI formation had strong nuclear TDP-IR (Stage 4, Figs. 5D, F). In Stage 4 mice, most of the nuclei were strongly positive and circular, but some weakly stained nuclei were atrophic or deformed (Fig. 4E). In G1H mice with a rapid disease course, TDP-IR of the neurons was weak, and nearly all LBHIs in the lumbar spinal cord were negative for TDP (Fig. 4F).

Statistical Analysis

The numbers of TDP-positive inclusions in neurons and glia were significantly lower in SALS patients with a

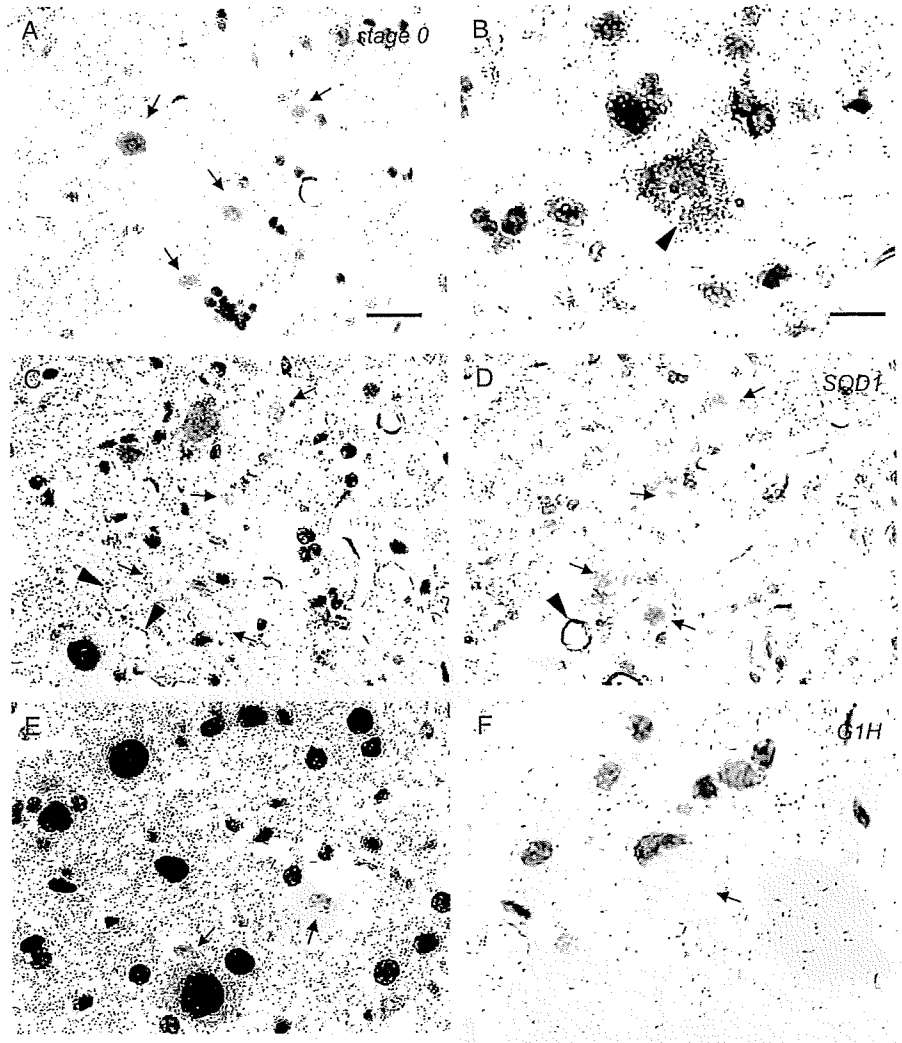

FIGURE 4. TAR DNA binding protein (TDP) pathology in G93A mice. **(A)** Nuclei in large neurons in a normal littermate (arrows) are TDP positive; their nucleoli are not stained. **(B–E)** G1L mice. **(B)** A degenerated neuron containing small vacuoles (arrowhead) in the cytoplasm has a TDP-negative nucleus and TDP-positive cytoplasm. **(C, D)** There are numerous Lewy body-like hyaline inclusions (LBHIs) that are TDP positive **(C)** and superoxide dismutase 1 (SOD1) **(D)** (arrows). Some vacuoles that are SOD1 positive **(D)** are partly stained for TDP (**C**, arrowheads). **(E)** Most of the nuclei in the neurons are strongly positive for TDP. A few nuclei that are stained only weakly (arrows) are atrophic and deformed. **(F)** The LBHI in the lumbar cord of the G1H mouse stains extremely faintly for TDP (arrow). **(A)** Normal littermate (Stage 0), **(B–E)** G1L mice, **(B–D)** Stage 3, **(E)** Stage 4, **(F)** G1H mouse. Immunohistochemistry for TDP **(A–C, E, F)** and SOD1 **(D)**. **(D)** is a serial section of **(C)**. Scale bars = **(A, C–E)** 50 μm; **(B, F)** 20 μm.

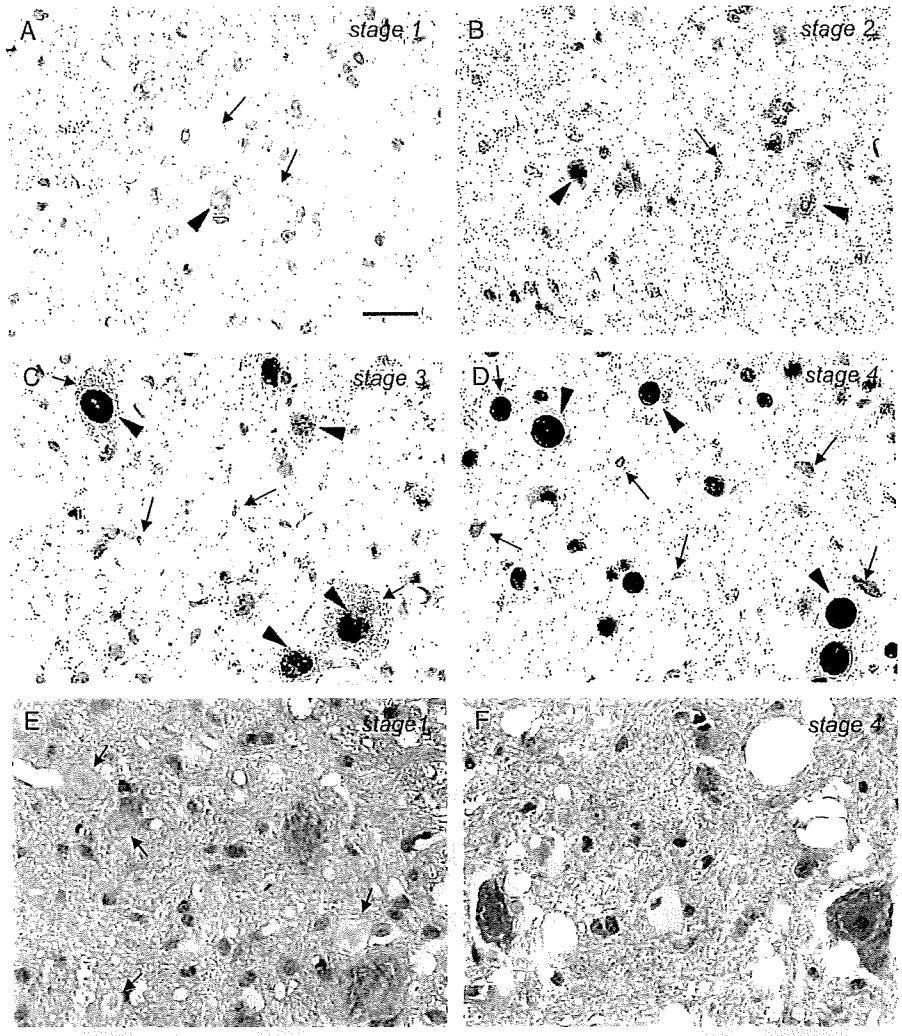

FIGURE 5. Four stages of TAR DNA binding protein (TDP) immunoreactivity in spinal cord neuron nuclei of G1L mice. **(A)** In Stage 1, nuclear immunoreactivity (arrowhead) is weak. Lewy body-like hyaline inclusions (LBHIs) (arrows) are only faintly stained or negative. **(B)** In Stage 2, nuclear immunoreactivity of neuron nuclei (arrowheads) is similar to that of normal littermates (Fig. 4A). Neurites or tiny vacuoles (arrow) also show immunoreactivity. **(C)** Immunoreactivity in Stage 3 in most of the nuclei (arrowheads) is stronger than in the normal control, but less than in Stage 4. There is diffuse and punctate cytoplasm staining and immunoreactivity in neurites (arrows). **(D)** Nuclear immunoreactivity in Stage 4 is very strong (arrowheads), and there are numerous TDP-positive neurites (arrows). **(E)** Prominent LBHIs (arrows) are evident in a Stage 1 mouse. **(F)** In a Stage 4 mouse, there are many vacuoles detected, but there is no LBHI formation. Immunohistochemistry for TDP (**A–D**); hematoxylin and eosin stain (**E, F**). Scale bar = 50 μm.

slow course than in those with a rapid course (Wilcoxon rank sum test: neuronal inclusions, p = 0.0002; glial inclusions, p = 0.0002). The numbers of large neurons (>37 μm) were also lower in SALS patients with a slow course than in those with a rapid course, although the level of significance (p = 0.0264) was lower than that for TDP-positive inclusions. The relationships among the numbers of large neurons, and TDP-positive inclusions in neurons and glia were not significant in SALS patients as a whole (Spearman correlation coefficient with 95% CI).

In G1L mice, the TDP-IR stage was positively correlated with life span (Spearman correlation coefficient with 95% CI, $r = 0.77$; 95% CI, 0.22–0.95) and negatively correlated with the formation of LBHIs ($r = -0.87$; 95% CI, −0.97 to −0.47). The correlation between life span and the number of LBHIs was also high ($r = -0.64$; 95% CI, −0.92 to 0.04). A cumulative probability plot of age at the end stage (Fig. 6) showed a higher value for the group with strong TDP-IR (Stages 3 and 4) than for those with weak TDP-IR (Stages 1 and 2); age at the end stage in the strong TDP-IR group was significantly greater than that in the weak TDP-IR group (Kolmogorov-Smirnov test, p = 0.015).

DISCUSSION

The TDP mislocalization from the nucleus to the cytoplasm was previously considered to be a disease-specific

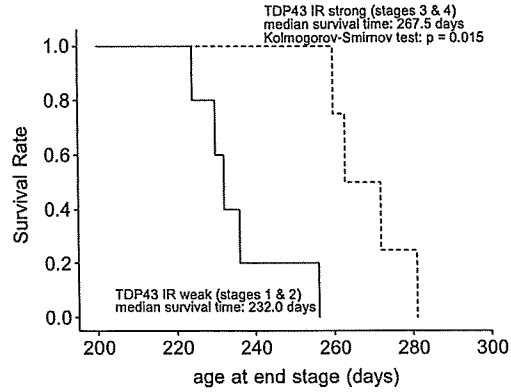

FIGURE 6. Kolmogorov-Smirnov test of the weak TAR DNA binding protein immunoreactivity (TDP-IR) groups (Stages 1 and 2) and strong TDP-IR groups (Stages 3 and 4) of G1L mice. Age at end stage in the TDP-IR strong group was significantly greater than that in the TDP-IR weak group ($p = 0.015$).

change not present in ALS1. Here, we analyzed TDP pathology in SALS and ALS1 patients and in ALS1 model mice. Our data suggest that the level of expression of TDP in the nucleus is associated with the clinical course and neurodegenerative changes in SALS patients and in ALS1 model mice.

Our observation that diffuse staining pattern was frequently observed in the cytoplasm of large neurons in SALS patients with rapid clinical courses showing mild neuronal loss suggests that TDP mislocalization starts gradually in the early phase of neurodegeneration. Most of the TDP-positive inclusions were found in atrophic neurons and glia, suggesting that the inclusions appeared later. Because no extracellular TDP-positive inclusions were apparent, neuronal TDP-positive inclusions likely disappear along with the death of the neurons.

In contrast, in SALS patients with slow clinical courses, no neurons with a diffuse TDP staining pattern in the cytoplasm were found, and TDP-positive inclusions in both neurons and glia were significantly less frequently found. Because relationships among the numbers of large neurons, those of TDP-positive inclusions in neurons, and those of TDP-positive inclusions in glia were not significant, the rarity of TDP pathology in SALS patients with a slow clinical course might not necessarily have resulted from severe neurodegeneration. The TDP pathology might be associated with a rapid clinical course in SALS. The influence of TDP-43 on the disease would then be less marked in SALS patients with a slow clinical course than in those with a rapid clinical course.

Previous studies have shown that LBHIs are not stained for TDP in ALS1 patients (16, 17, 26) and G1H mice (26).

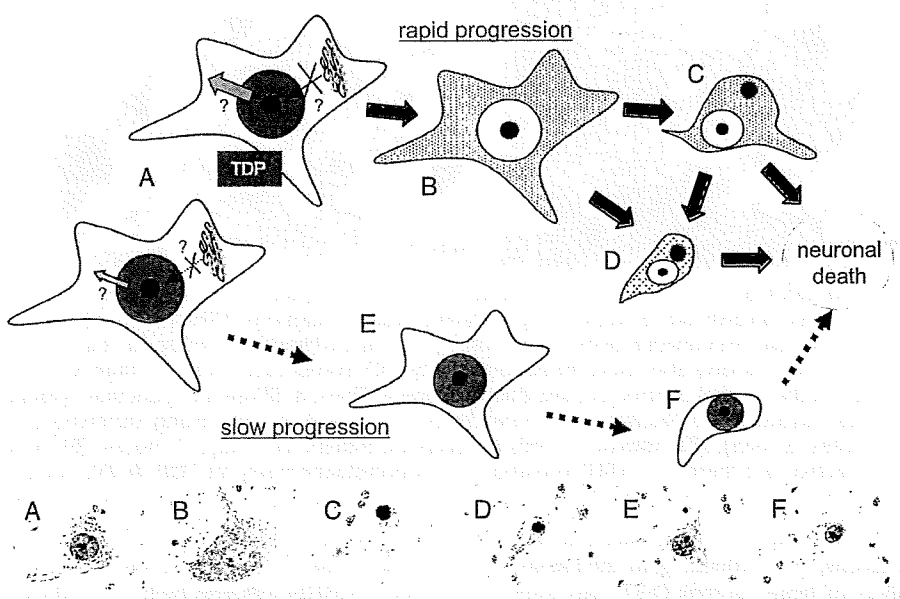

FIGURE 7. Hypothetical course of neuronal degeneration associated with changes in nuclear TAR DNA binding protein (TDP) expression in sporadic amyotrophic lateral sclerosis (SALS). **(A)** A morphologically normal neuron is subjected to an insult associated with a disturbance of TDP nuclear trafficking. The upper neuron diagrammed, from a patient with SALS, showing a rapid clinical course has marked disturbance of TDP nuclear trafficking, whereas the lower diagrammed neuron from a patient with SALS showing a slow clinical course, is only mildly affected. **(B–D)** Images show degenerating neurons at the time of rapid disease progression. **(B)** Early occurrence of TDP redistribution, i.e. low expression in nuclei and high expression in cytoplasm. **(C)** Later occurrence of cytoplasmic TDP aggregate in an atrophic neuron. **(D)** Similar aggregate of cytoplasmic TDP in a more degenerative neuron than that in **(C)**. **(E, F)** Images represent degenerative neurons at the time of slow disease progression. **(E)** Preservation of a high level of TDP expression in the nucleus of an atrophic neuron. **(F)** Successive maintenance of a high level of TDP expression in the nucleus of a more degenerative neuron. The lower 6 photographs are from SALS patients showing a rapid clinical course **(A–D)** and a slow course **(E, F)**, which correspond to the diagrammatic illustrations for each letter.

On the other hand, mislocalization of TDP to the cytoplasm in ALS1 cases (A4T, I113T) has been reported by Robertson et al (26). In the present study, TDP-positive LBHIs were clearly demonstrated in 1 ALS1 patient showing a slow disease progression, and in G1L mice, which also show slower disease progression than G1H mice. The ALS1 patients with TDP-negative LBHIs reported by Tan et al (17) showed very rapid progression within less than 1 year, and another ALS1 patient with TDP-negative LBHIs reported by Robertson et al (26) also showed rapid progression within 2 years. The difference in TDP immunoreactivity of LBHIs among ALS1 cases or between the 2 kinds of G93A mice might be a result of the difference in the clinical course or speed of SOD1 aggregation (34). The difference in morphology between TDP-positive inclusions in ALS1-1 and G1L mice and those in SALS patients would be caused by trapping of TDP-43 by SOD1 aggregation or LBHIs. The colocalization of TDP and SOD1 in LBHIs also suggests a biological relationship between SOD1 and TDP, although the specifics of that relationship are unclear.

Ayala et al (11) reported that loss of TDP in vitro results in nuclear dysmorphism, misregulation of the cell cycle, and apoptosis. Because the TDP-IR stage was positively correlated with life span in G1L mice, nuclei with low TDP-IR were atrophic and deformed in G1L mice and ALS1 patients, and an absence of TDP in the nucleus (such as that occurring through mislocalization) was frequently observed in SALS patients with a rapid clinical course, a high level of expression of nuclear TDP may play a protective role in neurons exposed to various insults. Because TDP-IR in the nucleus was inversely correlated with LBHI formation in G1L mice, TDP might have a suppressive effect on LBHI formation or toxic aggregation of SOD1, possibly through changes in the transcription and splicing of unknown genes (7, 8).

We hypothesized that rapid disease progression resulting from some insult to neurons might lead to disturbance of TDP nuclear trafficking (Fig. 7A) (35). Redistribution of TDP, with a low level of expression in the nucleus and a high level in the cytoplasm (Fig. 7B), occurs first, and cytoplasmic TDP later forms aggregates in the atrophic neurons (Figs. 7C, D). In contrast, neurons that succeed in maintaining a high level of expression of nuclear TDP (36) because of a slow shift of TDP (Fig. 7A, lower) show rather slower degeneration, and the disease progresses more slowly (Figs. 7E, F). It will be important to investigate the mechanism responsible for regulating the nuclear expression level of TDP, as this might yield a new strategy for treating not only ALS, but also other neurodegenerative disorders, including frontotemporal lobar degeneration.

ACKNOWLEDGMENTS

The authors thank T. Hamasaki and T. Sugimoto for their expert assistance with statistical analyses, and R. Yasui for technical assistance.

REFERENCES

1. Deng H-X, Hentati A, Tainer JA, et al. Amyotrophic lateral sclerosis and structural defects in Cu/Zn superoxide dismutase. Science 1993;261: 1047–51
2. Rosen DR, Siddique T, Patterson D, et al. Mutations in Cu/Zn superoxide dismutase gene are associated with familial amyotrophic lateral sclerosis. Nature 1993;362:59–62
3. Kato S. Amyotrophic lateral sclerosis models and human neuropathology: Similarities and differences. Acta Neuropathol 2008;115:97–114
4. Hadano S, Hand CK, Osuga H, et al. A gene encoding a putative GTPase regulator is mutated in familial amyotrophic lateral sclerosis 2. Nat Genet 2001;29:166–73
5. Yang Y, Hentati A, Deng HX, et al. The gene encoding alsin, a protein with three guanine-nucleotide exchange factor domains, is mutated in a form of recessive amyotrophic lateral sclerosis. Nat Genet 2001;29: 160–65
6. Buratti E, Brindisi A, Giombi M, et al. TDP-43 binds heterogenous nuclear ribonucleoprotein A/B through its C-terminal tail. J Biol Chem 2005;280:37572–84
7. Ayala YM, Pantano S, D'Ambrogio A, et al. Human, *Drosophila*, and *C. elegans* TDP43: Nucleic acid binding properties and splicing regulatory function. J Mol Biol 2005;348:575–88
8. Wang HY, Wang IF, Bose J, Shen CKJ. Structural diversity and functional implications of the eukaryotic *TDP* gene family. Genomics 2004;83:130–39
9. Buratti E, Baralle FE. Characterization and functional implications of the RNA binding properties of nuclear factor TDP-43, a novel splicing regulator of CFTR exon9. J Biol Chem 2001;276:36337–43
10. Mercado PA, Ayala YM, Romano M, et al. Depletion of TDP43 overrides the need for exonic and intronic splicing enhancers in the human apoA-II gene. Nucleic Acids Res 2005;33:6000–10
11. Ayala YM, Misteli T, Baralle FE. TDP-43 regulates retinoblastoma protein phosphorylation through the repression of cyclin-dependent kinase 6 expression. Proc Natl Acad Sci U S A 2008;105:3785–89
12. Kato S, Takikawa M, Nakashima K, et al. New consensus research on neuropathological aspects of familial amyotrophic lateral sclerosis with superoxide dismutase 1 (SOD1) gene mutations: Inclusions containing SOD1 in neurons and astrocytes. Amyotroph Lateral Scler Other Motor Neuron Disord 2000;1:163–84
13. Arai T, Hasegawa M, Akiyama H, et al. TDP-43 is a component of ubiquitin-positive tau-negative inclusions in frontotemporal lobar degeneration and amyotrophic lateral sclerosis. Biochem Biophys Res Commun 2006;351:602–11
14. Neumann M, Sampathu DM, Kwong LK, et al. Ubiquitinated TDP-43 in frontotemporal lobar degeneration and amyotrophic lateral sclerosis. Science 2006;314:130–33
15. Dickson DW, Josephs KA, Amador-Ortiz C. TDP-43 in differential diagnosis of motor neuron disorders. Acta Neuropathol 2007;114:71–79
16. Mackenzie IRA, Bigio EH, Ince PG, et al. Pathological TDP-43 distinguishes sporadic amyotrophic lateral sclerosis from amyotrophic lateral sclerosis with SOD1 mutations. Ann Neurol 2007;61:427–34
17. Tan C-F, Eguchi H, Tagawa A, et al. TDP-43 immunoreactivity in neuronal inclusions in familial amyotrophic lateral sclerosis with or without *SOD1* gene mutation. Acta Neuropathol 2007;113:535–42
18. Gitcho MA, Baloh RH, Chakraverty S, et al. TDP-43 A315T mutation in familial motor neuron disease. Ann Neurol 2008;63:535–38
19. Sreedharan J, Blair IP, Tripathi VB, et al. TDP-43 mutations in familial and sporadic amyotrophic lateral sclerosis. Science 2008;319: 1668–72
20. Cairns NJ, Neumann M, Bigio EH, et al. TDP-43 in familial and sporadic frontotemporal lobar degeneration with ubiquitin inclusions. Am J Pathol 2007;171:227–40
21. Amador-Ortiz C, Lin W-L, Ahmed Z, et al. TDP-43 immunoreactivity in hippocampal sclerosis and Alzheimer's disease. Ann Neurol 2007;6: 435–45
22. Nakashima-Yasuda H, Uryu K, Robinson J, et al. Co-morbidity of TDP-43 proteinopathy in Lewy body–related diseases. Acta Neuropathol 2007;114:221–29
23. Freeman SH, Spires-Jones TDP, Hyman BT, et al. TAR-DNA binding protein 43 in Pick disease. J Neuropathol Exp Neurol 2008;67:62–67
24. Lee EB, Lee M-Y, Trojanowski JQ, Neumann M. TDP-43 immunoreactivity in anoxic, ischemic and neoplastic lesions of the central nervous system. Acta Neuropathol 2007;115:305–11
25. Sanelli T, Xiao S, Horne P, et al. Evidence that TDP-43 is not the major ubiquitinated target within the pathological inclusions of amyotrophic lateral sclerosis. J Neuropathol Exp Neurol 2007;66:1147–53

26. Robertson J, Sanelli T, Xiao S, et al. Lack of TDP-43 abnormalities in mutant SOD1 transgenic mice shows disparity with ALS. Neurosci Lett 2007;420:128–32
27. Dal Canto MC, Gurney ME. A low expressor line of transgenic mice carrying a mutant *SOD1* gene develops pathological changes that most closely resemble those in human amyotrophic lateral sclerosis. Acta Neuropathol 1997;93:537–50
28. Parent A, Carpenter MB. *Carpenter's Human Neuroanatomy, 9th ed.* Philadelphia, PA: Lippincott, Williams &Wilkins, 1996
29. Sumi H, Nagano S, Fujimura H, et al. Inverse correlation between the formation of mitochondria-derived vacuoles and Lewy body–like hyaline inclusions in G93A superoxide dismutase–transgenic mice. Acta Neuropathol 2006;112:52–63
30. Kategawa J, Fujimura H, Ogawa Y, et al. A clinicopathological study of familial amyotrophic lateral sclerosis associated with two pair deletion in the copper/zinc superoxide dismutase (SOD1) gene. Acta Neuropathol (Berl) 1997;94:617–22
31. Kato S, Shimoda M, Watanabe Y, et al. Familial amyotrophic lateral sclerosis with a two base pair deletion in superoxide dismutase 1 (SOD1): Gene multisystem degeneration with intracytoplasmic hyaline inclusions in astrocytes. J Neuropathol Exp Neurol 1996;55:1089–101
32. Inoue K, Fujimura H, Ogawa Y, et al. Familial amyotrophic lateral sclerosis with a point mutation (G37R) of the superoxide dismutase 1 gene: A clinicopathological study. Amyotroph Lateral Scler Other Motor Neuron Disord 2002;3:244–47
33. Inoue K, Fujimura H, Toyooka K, et al. Familial amyotrophic sclerosis with L126S mutation of Cu/Zn superoxide dismutase gene. Pathological study of two cases [Abstract]. J Neurol 2006;235:120
34. Sato T, Nakanishi T, Yamamoto Y, et al. Rapid disease progression is correlated with instability of mutant SOD1 in familial ALS. Neurology 2006;65:1954–57
35. Winton MJ, Igaz LM, Wong MM, et al. Disturbance of nuclear and cytoplasmic Tar DNA binding protein (TDP-43) induces disease-like redistribution, sequestration and aggregate formation. J Biol Chem 2008; 283:13302–9
36. Wang IF, Chang HY, James Shen CK. TDP-43, the signature protein of FTLD-U, is a neuronal activity-responsive factor. J Neurochem 2008; 105:797–806

BRAIN and NERVE 60(8)：931-940，2008

総説

アルツハイマー病に対する新ワクチン療法
——現状とわれわれの試み

大倉良夫* 松本 陽*

Novel Vaccine Therapy for Alzheimer's Disease
—Recent Progress and Our Approach

Yoshio Okura*, Yoh Matsumoto*

Abstract

Alzheimer's disease (AD) is the most common cause of dementia with very few drugs available for its treatment. In 1999, Schenk et al reported that Aβ 1-42 peptide vaccination in AD model mice causes the reduction in Aβ deposits. Thereafter, a vaccine therapy was developed for the curative treatment of AD. Clinical trials of active vaccination for AD patients were halted due to the development of meningoencephalitis in some patients; however, vaccine therapy is thought to be effective based on the clinical and pathological findings of the vaccinated patients. Based on this information, active and passive vaccines have been developed, some of which are now urdergoing clinical trials in Europe and USA. However, there are still some problems for general application of such drugs for AD patients. Recently, we developed nonviral DNA vaccines and used them to obtain a substantial Aβ reduction in AD model mice without any side effects. In this article, we will review conventional vaccine therapies and introduce our non-viral DNA vaccine therapy. Finally, we will present data regarding the mechanisms of Aβ reduction after DNA vaccination. DNA vaccination for AD may open up new avenues in vaccine therapy for the treatment of AD.

Key words：Alzheimer's disease, nonviral DNA vaccine, Aβ reduction, microglial activation, phagocytosis by microglia

はじめに

アルツハイマー病は今から100年前，ドイツの精神医学者Alois Alzheimerにより最初に報告された神経疾患である。認知障害(記憶障害，見当識障害，学習の障害，注意の障害，空間認知機能，問題解決能力の障害など)を主症状として中年期以降に多発し，世界中で1,200万人を超える患者が存在すると考えられている[1]。発症後数年の経過を経て徐々に症状は進行し，重度になると摂食や着替え，意思疎通なども不可能となり，数年から十数年で寝たきりになり死に至る。経過中に被害妄想，幻覚や暴言・暴力・徘徊・不潔行為などの問題行動が出現することが多く，患者本人ばかりか家族や介護者を含めて大きな社会問題となっている。

Ⅰ．アミロイド仮説

アルツハイマー病は，肉眼病理的に高次機能をつかさどる前頭葉，前頭葉連合野や側頭葉，海馬領域の中等度から高度の脳萎縮によって特徴付けられ，大脳皮質や海馬の萎縮を反映して脳室は拡大する。顕微鏡レベルでは，

* 東京都神経科学総合研究所分子病理学部門〔〒183-8526 東京都府中市武蔵台2-6〕Department of Molecular Neuropathology, Tokyo Metropolitan Institute for Neuroscience, 2-6 Musashidai, Fuchu, Tokyo 183-8526, Japan

1881-6096/08/¥500/論文/JCLS

Table 1 Viral vs Nonviral DNA vaccines

	Nonviral	Viral
Advantage	• **Safe** • **Mass-producible** • **Low cost**	• Inducible to particular cells • High induction efficiency
Disadvantage	• Low induction efficacy	• **Possibilities of tumorigenecity or leukemia** • **Possibilities of adverse effects (immunogenicity, cytokine storms)** • **Difficulty in mass production**

老人斑，神経原線維変化(neurofibrillary tangle)，神経細胞脱落の3つの特徴がある。アミロイドの蓄積がタウや神経細胞の変化に先行することは多くの研究により報告され，非認知症老人やダウン症の剖検脳でも観察されている。近年，アミロイドの沈着がこの病態の最上流に位置しアミロイドの蓄積を防止できるならば，その後に起きる事象，すなわち，神経細胞内のタウの蓄積，神経細胞の脱落などをある程度防ぐことができるとする「アミロイド仮説」が広く受け入れられるようになった[2]。

II．ワクチン療法の開発　能動免疫療法

アミロイド仮説をもとに，1999年Schenkらによりアルツハイマー病の根治的治療法としてAβペプチド・ワクチン療法が提唱された[3]。彼らは，体外からAβペプチドを免疫賦活剤（アジュバンド）とともに投与し，体内で抗Aβ抗体の産生を誘導し，脳内のAβ蓄積が減少することをアルツハイマーモデルマウスで証明した。その後，脳内の病理学的所見のみならず学習記憶能力もワクチン投与により改善されることが明らかになり[4,5]，欧米においてAβワクチン（Aβ1-42アジュバンド）のヒト臨床試験が開始されることとなった。Elan社にて製造された合成Aβ42製剤であるBetabloc（AN-1792）を用いた第I相試験（安全性試験）では，約100例の軽度から中等度のアルツハイマー病の患者に投与された。この試験は重要な副作用もなく終了し，投与された患者の血清中に抗Aβ抗体が生体内で合成されたことが確認された[6]。第I相試験に引き続きアメリカとヨーロッパの30の施設において軽度から中等度のアルツハイマー患者に対して第II相試験（二重盲検試験）が行われた。しかし実薬投与を受けた298例のうち18例（6％）に髄膜脳炎が発症し，障害を残す重症症例も出たため，2002年1月に治験自体が中止された[7]。ワクチンの免疫活性化作用によりTリンパ球などの組織障害性細胞性免疫が惹起され，一部の患者でAβに反応するTh1型CD4陽性細胞が脳に浸潤し，アレルギー性実質的脳脊髄炎のような髄膜脳炎を引き起こしたのではないかと推察された。

臨床試験は不満足な結果に終わったものの，その後の検索によってワクチン治療が有益であるという重要な所見が示された。2003年，ワクチン投与を受けた患者の最初の剖検例が報告された[8]。症例は72歳の女性で5年間の緩徐進行性の記憶障害の経過があり，AN-1792（pre-aggregated Aβ 42; 50 μg）を5回投与された後，2001年5月から脳炎症状が出現した。投薬は直ちに中止され脳炎の治療が行われたものの，寝たきりとなり20カ月後の2002年2月に肺梗塞のため死亡した。脳病理はBraak stage V-VIのアルツハイマー病の所見であった。脳炎の所見として髄膜，髄膜血管周囲および大脳皮質へのT細胞とマクロファージの浸潤が認められ，大脳白質には髄鞘線維の減少が認められた。しかしその一方，新皮質では老人斑が消失し，それに伴うアストロサイトの増殖や変性軸索も消えていた。老人斑が消失している部位ではAβ分解産物を貪食したミクログリアの像も認められ，この所見からワクチンがヒトのアルツハイマー病においても老人斑の減少効果があると推測された。さらにその後，Gilmanらは臨床試験の抗Aβ抗体の抗体価と高次機能の改善について最終報告を行った[9]。ワクチン投与300名中59人が抗体陽性であり，陽性群では各種高次機能試験のうちneuropsychological test battery (NTB)で有意の改善を認めた。これらの事実は，能動免疫療法により一部患者に脳内炎症症状が出現したものの，ワクチンによるAβ減少効果がヒトアルツハイマー病症例においても認められることを示すものであり，過剰な免疫反応を抑制することができれば，ヒトにおいてもワクチン療法が有効である可能性が高いことを示唆している。

臨床治験後，脳炎を惹起しないようなワクチン薬剤を作ることを目標として薬剤開発が行われている。Aβペ

プチドはそのC（カルボキシル）末端側フラグメントが主としてTh1反応を誘導し，N（アミノ）末端側フラグメントがTh2反応を誘導することがわかっている[10]。そこで，Elan社はAβのN末端側フラグメントをキャリア蛋白質に結合させたワクチンを開発し，このワクチンを用いた治験を開始している[11]。そのほか，キャリア蛋白質を使用しないN末端フラグメントワクチンとしてAβ1-15ペプチド2本をリジン残基でつないだものが作られ，アルツハイマー病モデルマウスでその有効性が確認されている[12]。Th1反応を起こしにくいとされる粘膜免疫反応を使って，抗体産生を誘導するワクチンも開発されている[13]。しかし，能動免疫療法はアジュバントを必要とするために，脳炎などの副作用を完全に克服することは現時点で難しいと考えられる。

Ⅲ．受動免疫療法

抗Aβ抗体を直接体内に投与する受動免疫療法は，能動免疫療法に代わりうる方法であり，早い段階から能動免疫療法と並行して開発が進められている。末梢から抗Aβ抗体を投与することにより，アミロイド斑の減少が認められており，さほど高濃度でなくとも脳内に入りアミロイド斑の減少効果があることがわかっている[14,15]。最近の研究ではAβ蛋白のN末端が抗体認識部位として重要であることが示され，これは凝集したAβのN末端が突出し，抗体が認識しやすいからであると考えられている。受動免疫療法の最大の利点は免疫賦活剤を使用しないことであり，そのため能動免疫療法のヒト臨床試験で問題となった過剰な細胞免疫が誘発されにくい。既に欧米においてElan-Wyeth社のヒト化モノクローナル抗体（AAB-001）のヒト臨床試験が第III相試験まで進行している。国内においても順天堂医院において治験参加者が募集されており，近日，第I相試験が予定されている。

しかし受動免疫療法には，投与された抗Aβ抗体はアミロイド斑のみならずアミロイドが沈着している血管にも結合して血管壁の脆弱化を促進し，出血をきたすことが報告されていること[16]，投与された抗体に対して抗体が産生され（抗イディオタイプ抗体）複数回の投与により効果が減弱，ないしは消失する可能性があることなどクリアしなければならない課題も多い。さらに，受動免疫療法は抗ヒト型抗体の製作費用が高いために，治療費が莫大な額になることが予想されており，それにより治療が不可能となるケースが出るであろうと考えられている。

Ⅳ．次世代に向けた新しいワクチン療法 ——DNAワクチンの開発

これらに代わるアルツハイマー病の新ワクチン治療として，開発されたのがDNAワクチン療法である。DNAワクチンは遺伝子を運ぶベクター（プラスミドやウイルス）にAβ蛋白を作らせる遺伝子を組み込んで投与し，ワクチンを取り込んだ細胞にAβ蛋白を作らせる。産生されたAβは免疫系を刺激し，抗Aβ抗体を誘導する（Fig. 1）。DNAワクチンは，投与後で長時間体内にとどまり，コードされたペプチドを緩徐に作り続けるために過剰な免疫反応を避けることが可能で，単純な構造であるため簡単に改良することができる。[17,18]。さらに，宿主に誘導される免疫反応はTh2型であるという利点がある[17,19,20]。

いくつかのグループから，アデノウイルスベクター[21]，アデノ随伴ウイルスベクター（AAV）[22,23]などのウイルス性ベクター用いてワクチンを開発した報告がなされた。Zhangらは，AAVワクチンを1回のみ投与することにより長期間抗Aβ抗体がアルツハイマーモデルマウスに誘導され，脳内のAβ沈着が減少し，記憶認知能力が改善することを報告した[22]。さらにKimらは，アデノウイルスベクターに組み込んだGM-CSFおよび11 tandem repeats of Aβ 1-6を同時投与することにより，高い抗体価が得られたことを報告した[21]。しかしながら，アデノウイルスやアデノ随伴ウイルスは悪性腫瘍を誘発する可能性が完全に否定することができない（後述）[24,25]。また，AAVベクターを患者治療に用いる量までにスケールアップするのは非常に困難で，商業利用できるレベルではないこと[26]などから，ウイルス性ベクターを用いたDNAワクチンを臨床応用することは，現在のところ障害が大きい。

一方，非ウイルス性のプラスミドベクターを用いてDNAワクチンを作製した報告も認められる。プラスミドベクターによる非ウイルス性DNAワクチンは低いコストにより大量生産が可能であり[17,18]，ウイルス感染や形質転換の危険性がない[27,28]などの利点がある。Ghochikyanらは，非ウイルス性プラスミドベクター中にAβ1-42とTh-2 cytokineであるIL-4 sequenceを導入し，wild type B6マウスに抗Aβ抗体を誘導した[29]。Schiltzらは分泌シグナルである組織プラスミノーゲンアクチベーターの遺伝子を含むDNAワクチンを低用量のAβ蛋白と同時投与することにより，アルツハイマーモデルマウスの脳内Aβの減少に成功した。しかしDNAワク

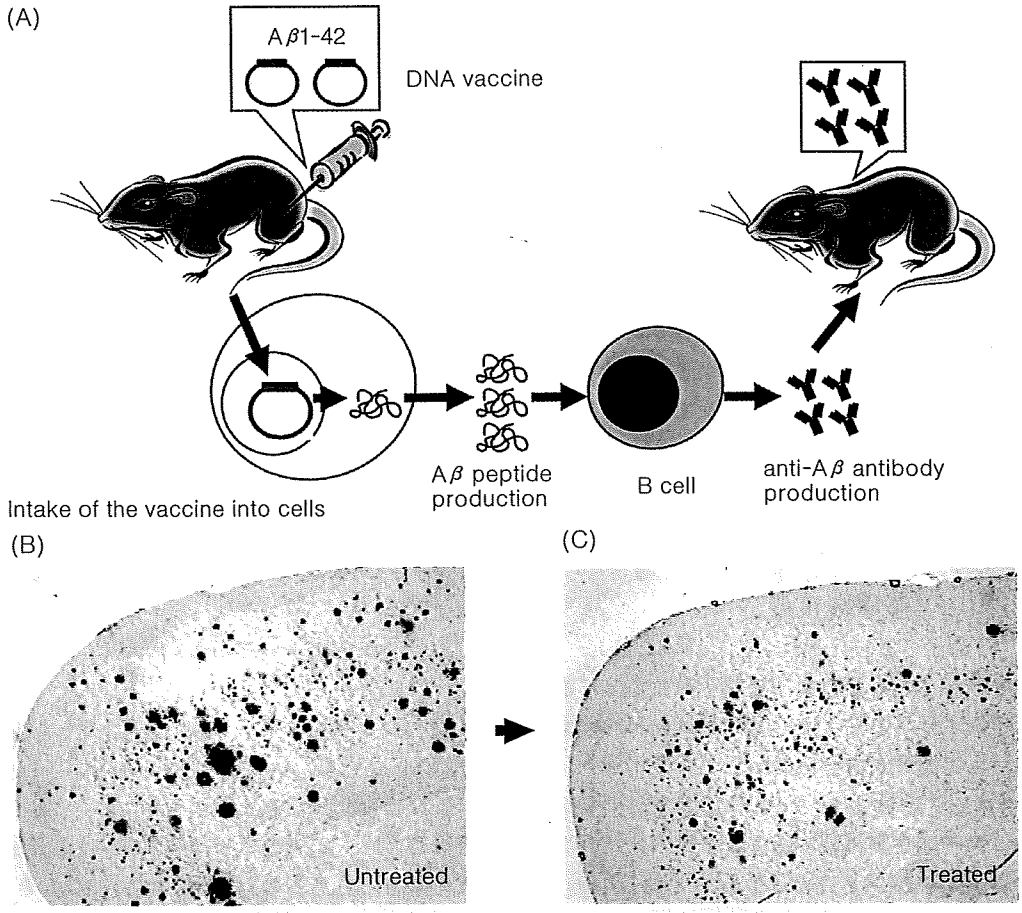

Fig. 1 Schematic representation of Aβ reduction by DNA vaccination

Plasmid vectors encoding Aβ 1-42 are injected intramuscularly to generate Aβ peptides and subsequent anti-Aβ antibodies. Aβ peptide production is maintained by muscle cells over a certain period (A). Amyloid plaques of various sizes were detected in the frontal cortex of untreated mice (B). Therapeutic administration of Aβ-Fc vaccines reduced cortical Aβ burden at 15 months (C).

チン単独で脳内 Aβ の減少を誘導することはできなかった[30]。

われわれの研究室では，これまでラットの実験的脳脊髄炎（EAE）などの自己免疫疾患モデルに対し非ウイルス性DNA ワクチンを作製し，その効果を報告してきた[31]。そのデータの蓄積をもとに，哺乳類細胞発現ベクターに Aβ-protein(1-42)および付属のシークエンスを挿入して 3 種類のアルツハイマー病非ウイルス性 DNA ワクチンを作製した。① Aβ 1-42 のみを挿入したもの（K-Aβ ワクチン），②発現蛋白質の分泌を向上させるためにマウス Igκ シグナルを付加したもの（IgL-Aβ ワクチン），③分泌した蛋白質の安定性を向上させるために Immunoglobulin の Fc 領域を付加したもの（Aβ-Fc ワクチン），の 3 種類である。3 種類のベクターを HEK293T に transfect し，その細胞内に Aβ1-42 ペプチドが発現し，培養上清に分泌されているか否かを ELISA 法により検討した。IgL-Aβ，Aβ-Fc ワクチンは培養上清中に Aβ 1-42 ペプチドが分泌されていた。Aβ1-42 のみを挿入した K-Aβ ワクチンは Aβ 1-42 ペプチドの分泌が認められなかった。その後，K-Aβ ワクチンは Aβ 抑制効果が他の 2 つのワクチンに比べて低いことがわかったので，詳細な検討から除外した。

作製した DNA ワクチンをアルツハイマー病のモデルマウス（APP23 Tg mouse）に 2 週間に 1 回，投与することにより治療を試みた。このモデルマウスは，スウェーデンの家族性アルツハイマー病家系にみられる遺伝子変異を持つアミロイド前駆蛋白が遺伝子導入されており，6 カ月齢から老人斑が出現し，加齢とともに増加するこ

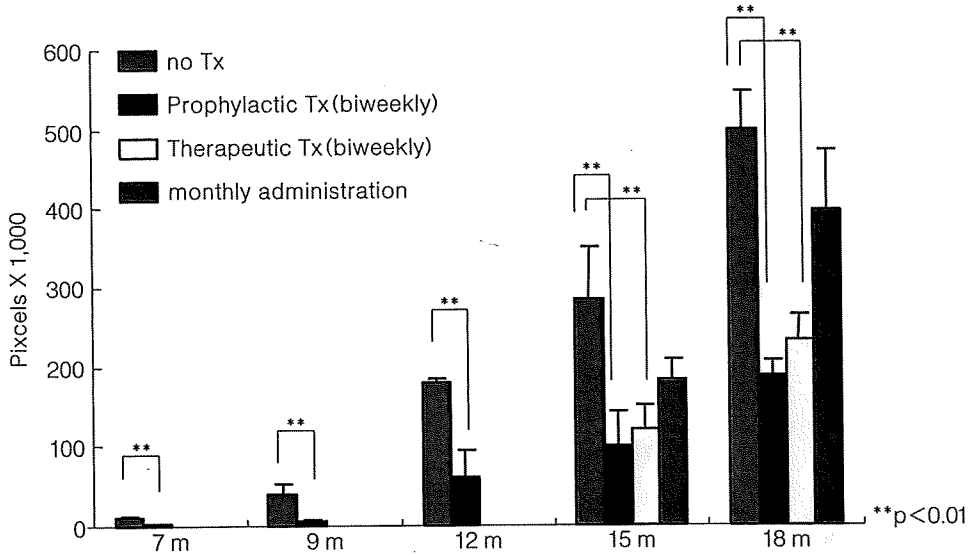

Fig. 2 Summary of quantitative analysis of Aβ burden in treated and untreated model mice

Blue, yellow, red and green bars represent the Aβ burden in untreated mice and in mice treated prophylactically treated (biweekly), therapeutically (biweekly) and monthly, respectively. Amyloid deposition was first detected in untreated mice at 7 months (7m) of age, and it was observed to rapidly increase after 15 months of age. Aβ deposition was significantly reduced in mice treated with DNA vaccine biweekly as compared with untreated control mice. Prophylactic administration of Fc-Aβ vaccine prevented Aβ deposition by 10-30% of that in untreated animals at 12 months of age and to 40-50% at 15 months. The effects of therapeutic administration were almost the same as those of prophylactic administration. Aβ reduction in mice treated monthly was lower than that in mice treated biweekly.

とがわかっている。ワクチン投与後，マウスの脳を免疫組織化学染色し，沈着したAβを画像解析した。Aβ沈着がまだ出現していない3～4カ月齢からワクチンを投与した予防的投与群（Fig. 2 red bars）においては70～90%，既にAβ沈着が認められた12カ月齢から治療的にワクチンを投与した治療的投与群（Fig. 2 yellow bars）においては50～60%のAβ沈着が，コントロール群（Fig. 2 blue bars）に比較し有意に減少していた。ワクチンの効果は投与回数に依存する傾向があり，1カ月に1度投与した場合Aβの減少効果は減弱した（Fig. 2 green bars）。DNAワクチン投与後の脳を免疫組織化学的に詳細に検索したが，Aβペプチド・ワクチンを投与したときにみられる，T細胞や炎症細胞の浸潤などの脳髄膜炎を思わせる所見はまったく認められなかった。さらにモデルマウスと同系で遺伝子操作を行っていないマウスにワクチンを投与し，そのリンパ節細胞からT細胞を分離しAβペプチドへの反応性を細胞増殖試験で解析したが，抗原反応性T細胞の活性化はまったく誘導されていなかった。これらの所見からDNAワクチンによる過剰な免疫反応はほとんどなく，Aβを減少する効果があると考えられた[32]。

V. アルツハイマー病に対する免疫療法の安全性

アルツハイマー病は数年から十数年の経過でゆっくり進行する。このため患者の治療を行う場合，長期に投与する必要性が高く，薬剤の安全性が強く求められる。能動免疫療法においては，脳炎などの過剰な免疫反応を惹起しないような薬剤を作製することが，今後のワクチン開発の課題になるであろう。また受動免疫療法では，抗体投与後に脳出血が起こる可能性があること，抗イディオタイプ抗体が産生され複数回の投与により効果が減弱する可能性があること，治療費が莫大になることなどに注意する必要がある。

DNAワクチンは，脳内の過剰な細胞免疫反応が誘導されにくく，能動免疫療法，受動免疫療法の欠点を克服できる可能性が高いが，遺伝子の導入に伴うベクターの安全性に留意する必要がある。遺伝子治療は，1990年に米国で先天的免疫不全であるADA欠損症の患者を対象

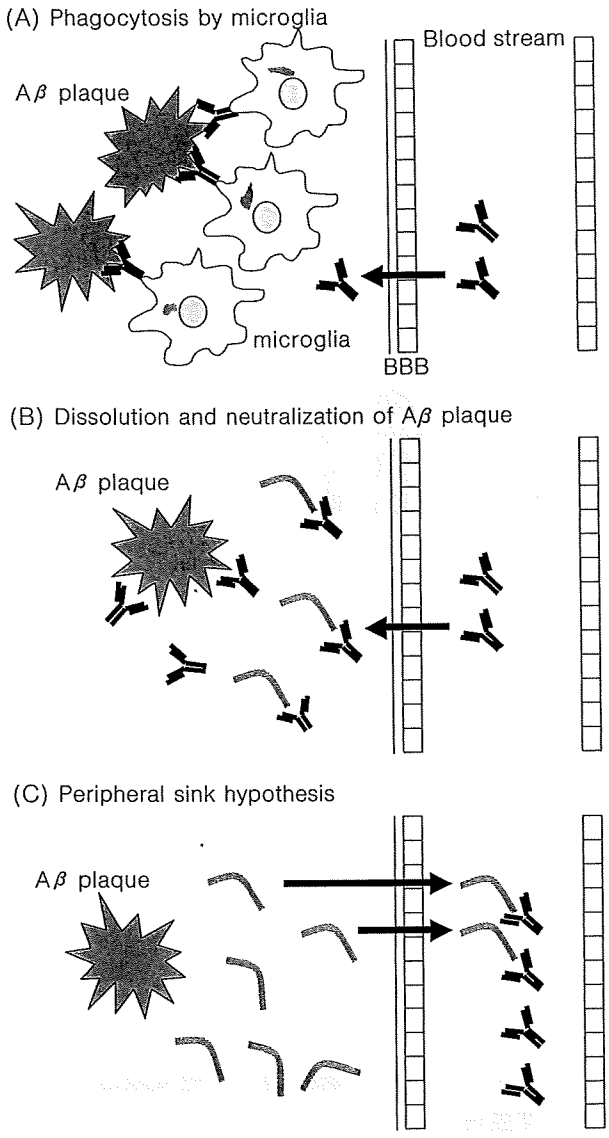

Fig. 3 Mechanisms of amyloid reduction with vaccine treatment

There are 3 hypotheses that can explain the amyloid reduction after vaccine therapy. (A) Phagocytosis by microglia: Anti-Aβ antibodies traverse the blood-brain barrier (BBB) and attach to Aβ deposits, which leads to Fc receptor-mediated phagocytosis by microglia. (B) Dissolution of Aβ plaques: antibodies bind to the N-terminus of Aβ deposits and dissolve amyloid fibrils. (C) The peripheral sink hypothesis: anti-Aβ antibodies in the circulation induce a net efflux of Aβ from the brain to plasma

にしてレトロウイルスベクターで実施されて以来，その有効性を拡大し，癌，HIV などを対象に，世界で約 4,000 例が行われ，治療として確立した感があった。しかし 1999 年にペンシルバニア大学の Wlison らにより実施されていた先天性代謝疾患（OTC 欠損症）の臨床試験で，大量のアデノウイルスを肝動脈から全身投与した 18 歳の男性患者が肝臓障害で死亡する事故が起こった。遺伝子治療で初の死亡例と報告されて以来，安全性に対する見直しが行われている[33]。その後，レトロウイルスベクターについても，フランスで 1999 年から X 連鎖重症複合免疫不全症（X-SCID）に対して実施された遺伝子治療の患者 11 人に関して，2002 年から 2003 年にかけて 3 人に有害事象（白血病の発症）が報告され，X-SCID の遺伝子治療が一時凍結状態になった[34]。さらに，非病原性で安全性が高いと考えられていた AAV ベクターに関しても，長期投与した場合の tumorigenecity が報告されている[35]。また，マウスに肝細胞癌を引き起こすという報告も認められる[36]。確率は極めて低いと考えられるものの，このような深刻な事態の出現は従来安全とされてきたウイルスベクターの安全性に関して，再度慎重な検討を行う必要性が出てきたことを示している。

これに対して，非ウイルス性ベクターは，特定の細胞に遺伝子を導入できないこと，導入効率が悪いことなどの欠点はあるものの，宿主細胞染色体への integration は 15 万回に 1 回程度で，自然突然変異とほぼ同程度の無視できる割合であり[37]，安全性についてはほぼ確立されている。現時点ではアルツハイマー病の DNA ワクチン療法のベクターとして非ウイルス性プラスミドベクターが最善であると思われる。

VI. DNA ワクチンの作用機序

アルツハイマー病ワクチン療法における β アミロイド除去の機序として，現在以下の 3 つの説がある[6]。第 1 は，抗 Aβ 抗体が凝集した Aβ に結合し，Fc receptor を介してミクログリアに貪食されるために老人斑が除去されるという説である（Fig. 3 A）[38,39]。第 2 は抗 Aβ 抗体が Aβ の N 末のアミノ酸を主に認識して結合し，凝集不溶化した Aβ を可溶化し，さらに分泌された Aβ の凝集沈着を抗体が抑制することによりアミロイド沈着を減少させるという説である（Fig. 3 B）[40,41]。第 3 は Aβ に対する抗体は血液脳関門を越えず，末梢血末梢組織において Aβ を減少させることにより脳組織から髄液を経由して Aβ を末梢血中に引き出すという，peripheral sink 仮説である（Fig. 3 C）[15,42,43]。今回，筆者らの DNA ワクチン投与の系で，これらの仮説が成り立つか否かを検証した。

まず DNA ワクチン投与後のミクログリアの活性化の程度を知るために，ワクチン投与したマウスと対照群のマウスの脳切片を Iba-1（microglia surface marker，茶色）と 6F/3D（anti-Aβ 8-17，青）で二重染色し，病理

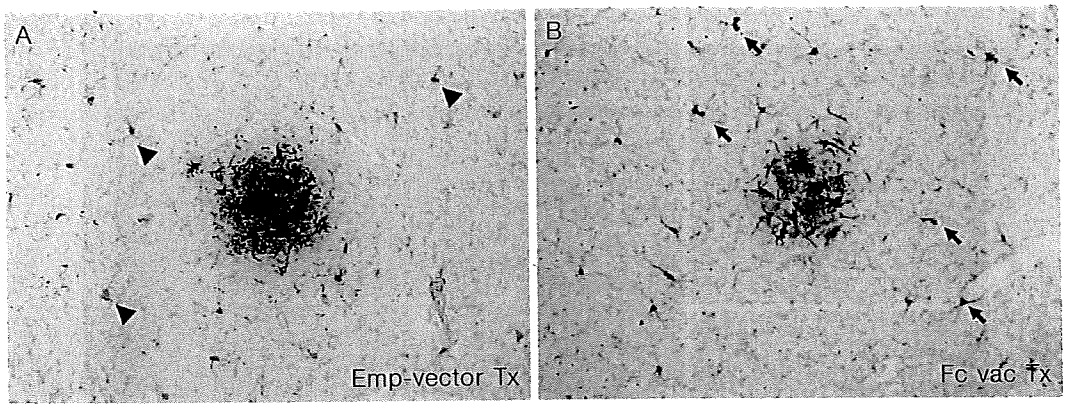

Fig. 4 Double staining with 6F/3D (amyloid plaques, blue) and Iba-1 (microglia, brown) in the brains of treated and untreated mice

Microglia with rich cytoplasms and processes with bulbous swellings are observed surrounding the plaques in the brains of untreated mice (A). After the treatment, more microglial cells infiltrated the amyloid plaques (B). In the remote brain regions of the non-treated APP23 mice, resting microglia were sparsely distributed (arrow heads in A). In the remote area of treated APP23 mice, microglial cells also increased in number and were present in the activated form (arrows in B).

学的解析を行った。この結果，野生型のＢ６マウスにおいては，小さな細胞質と細い突起を持つ休止型ミクログリアが脳全体に分布していた。未治療のモデルマウス(APP23)では，アミロイド斑周囲領域(periplaque area)に，大きな細胞質と太い突起を持つ活性化ミクログリアがアミロイド斑周囲に認められ，ミクログリアの突起はアミロイド斑に入り込んでいた。アミロイド斑から離れた領域 (remote area) ではミクログリアは野生型Ｂ６マウスで観察されたように休止型であり，活性化像は認められなかった(Fig. 4 A)。これに対して治療群のモデルマウスでは，periplaque area のミクログリアはアミロイド斑の周囲で塊状となって有意に数を増しており ($p<0.01$)，remote area でもミクログリアはその数を増して活性型に変化していた (Fig. 4 B)。ミクログリアの数の増加の割合は periplaque area よりも remote area で大きかった。

二重染色においてミクログリア内にアミロイドを認めることがしばしばあり，ミクログリアの貪食能が亢進している可能性が考えられた。それを定量的に分析するため，共焦点顕微鏡を用いてミクログリアの貪食能の変化を調べた。共焦点顕微鏡による観察では Cy3 でラベルされたミクログリア (赤) の中に，FITC ラベルされた Aβ 沈着 (緑) が観察された (Fig. 5)。三次元解析をすることにより Aβ 沈着がミクログリア内にあることを確認した。アミロイドを貪食したミクログリア数は，ワクチン投与群で有意に増加していた ($p<0.01$)。さらに，治療群でアミロイド斑表面に付着する抗体が増加することを免疫組織学的方法で確認した。

ミクログリアは，あるときは神経保護的に，あるときは神経損傷的に作用することが知られている。ワクチン投与後のミクログリアの増加がどちらの場合にあたるのかを，神経障害性サイトカインである TNF-α[44] を指標にして推測した。LPS 処理マウスおよび MOG-EAE－誘導マウスでは TNF-α が著明に増加していたものの，ワクチン投与後の増加は認められなかった。増加したミクログリアは神経保護的に作用しているものと考えられた。近年，oligomer として存在する可溶性 Aβ (soluble Aβ) に，シナプス障害等の神経細胞障害作用があることが報じられているが[45]，筆者らの系においてもワクチン投与により脳内の oligomer が減少することが western blotting 法により確かめられており，特に remote area の活性型ミクログリアの増加は，Aβ oligomer の除去に関与しているものと考えられた。

さらに，DNA ワクチンによって誘導された抗 Aβ 抗体が直接 Aβ 沈着に結合し，これを解離して除去する可能性[46]についても検討した。これは直接的評価が難しく，以下の手法でその程度を推測した。治療群および未治療群のマウス血清がアルツハイマー病モデルマウスのアミロイド斑と結合するか，否かを tissue amyloid plaque immunoreactivity (TAPIR)にて検討した。治療群の抗 Aβ 抗体は未治療群の抗体に比較して抗体価が高かったものの，Aβ に対する結合反応は著明ではなかった。抗体による Aβ の直接的解離，可溶化作用はさほど強くないと考えられた。次に，脳内から末梢血中に Aβ の

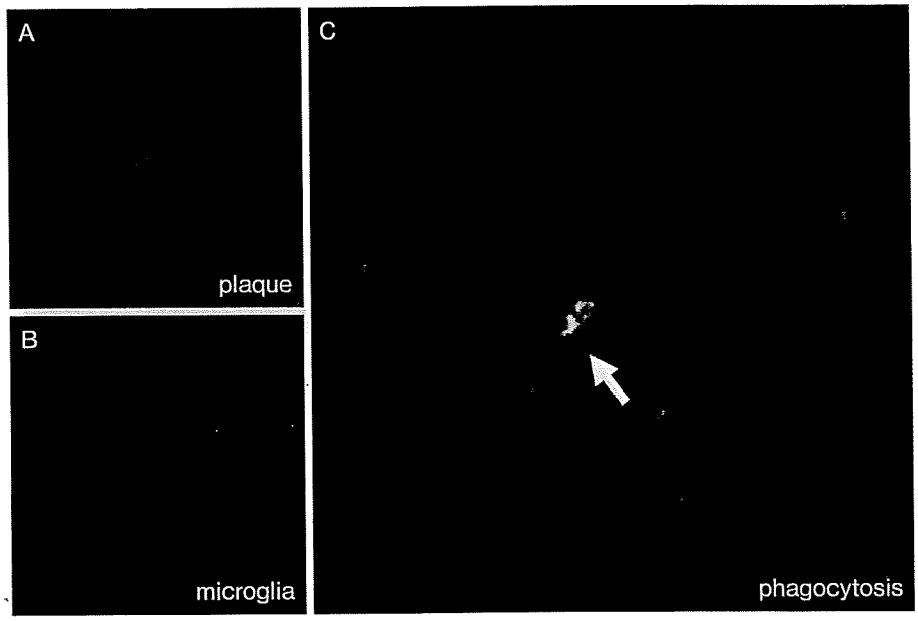

Fig. 5 Phagocytosis of Aβ deposits by activated microglia
Brain sections from treated APP23 mice were stained with 6F/3D (amyloid plaques, green) (A) and Iba-1 (microglia, red) (B) and observed with a confocal microscope. Single microglia present in remote brain region contain Aβ deposits (arrows in C).

引き抜きが起こっている可能性（peripheral sink hypothesis）を知るために，治療群および未治療群のマウスの血漿Aβを測定した。9カ月齢のマウスでは，治療群の一部で血漿Aβ量が高値であり，脳から血液へのAβの移行が亢進していると考えられた。しかし，15カ月齢では，治療群および未治療群で血漿Aβ値に変化はなかった。血管のアミロイド沈着が軽微な9カ月齢ではワクチン投与後，引き抜きが亢進している可能性がある。しかし15カ月齢では血管内のアミロイド沈着が進行し，引き抜きがほとんど起こらないことを示している。この機序はDNAワクチン療法では主要なルートではないと考えられた。

これらの事実から，DNAワクチン投与後のAβの除去はミクログリアによるAβの貪食によるところが大きく，抗Aβ抗体の直接作用や引き抜き作用の関与は存在しても弱いと考えられた。DNAワクチンはベクター内の遺伝子配列を変えることにより，簡単に再構成することができる。今後，さらに効果が高く副作用が少ないワクチンを開発発展する場合において有益である。

おわりに

コリンエステラーゼ阻害薬の塩酸ドネペジル（商品名アリセプト）は日本で唯一認可を受けたアルツハイマー病治療薬であり，症状の進行を遅らせることが知られている。しかし，効果は限定的で根治には至らないため，根本的な治療法の開発が社会的に極めて重要な課題であった。筆者らの作製したDNAワクチンがAβ沈着を有効に削減し，低価格で高い安全性を示したことが新聞，テレビなどで報道され，患者およびその家族からの多数の問い合わせが寄せられた。いかにアルツハイマー病が切実な問題であるか，ということを示していると言えよう。社会的反響を受け，現在筆者らの研究室では，プラスミド内に抗体産生を増加させるペプチドやミクログリアの貪食能を増進するペプチドを加え新たな数種類のワクチンを試作し，その効果を検討中である。さらに，創薬および臨床応用を具体的に視野に入れ，早期に医薬品製造管理基準（Good Manufacturing Practice: GMP）に対応した施設でヒト型DNAワクチンを製造しつつある。その後，医薬品の臨床試験の実施に関する基準（Good Clinical Practice: GCP）に沿い前臨床，および臨床試験を実施する予定にしている。

文　献

1）Citron M: Alzheimer's disease: treatments in discovery and development. Nat Neurosci **5 Suppl**: 1055-1057, 2002

2) Hardy J, Allsop D: Amyloid deposition as the central event in the aetiology of Alzheimer's disease. Trends Pharmacol Sci **12**: 383-388, 1991
3) Schenk D, Barbour R, Dunn W, Gordon. G, Grajeda H, et al: Immunization with amyloid-beta attenuates Alzheimer-disease-like pathology in the PDAPP mouse. Nature **400**: 173-177, 1999
4) Morgan D, Diamond DM, Gottschall PE, Ugen KE, Dickey C, et al: A beta peptide vaccination prevents memory loss in an animal model of Alzheimer's disease. Nature **408**: 982-985, 2000
5) Janus C, Pearson J, McLaurin J, Mathews PM, Jiang Y, et al: A beta peptide immunization reduces behavioural impairment and plaques in a model of Alzheimer's disease. Nature **408**: 979-982, 2000,
6) Hock C, Konietzko U, Papassotiropoulos A, Wollmer A, Streffer J, et al: Generation of antibodies specific for beta-amyloid by vaccination of patients with Alzheimer disease. Nat Med 8: 1270-1275, 2002
7) Orgogozo JM, Gilman S, Dartigues JF, Laurent B, Puel M, et al: Subacute meningoencephalitis in a subset of patients with AD after Abeta42 immunization. Neurology **61**: 46-54, 2003
8) Nicoll JA, Wilkinson D, Holmes C, Steart P, Markham H, et al: Neuropathology of human Alzheimer disease after immunization with amyloid-beta peptide: a case report. Nat Med **9**: 448-452, 2003
9) Gilman S, Koller M, Black RS, Jenkins L, Griffith SG, et al: Clinical effects of Abeta immunization (AN1792) in patients with AD in an interrupted trial. Neurology **64**: 1553-1562, 2005
10) Maier M, Seabrook TJ, Lemere CA: Developing novel immunogens for an effective, safe Alzheimer's disease vaccine. Neurodegener Dis **2**: 267-272, 2005
11) Masters CL, Beyreuther K: Alzheimer's centennial legacy: prospects for rational therapeutic intervention targeting the Abeta amyloid pathway. Brain **129**: 2823-2839, 2006
12) Maier M, Seabrook TJ, Lazo ND, Jiang L, Das P, et al: Short amyloid-beta (Abeta) immunogens reduce cerebral Abeta load and learning deficits in an Alzheimer's disease mouse model in the absence of an Abeta-specific cellular immune response. J Neurosci **26**: 4717-4728, 2006
13) Frenkel D, Maron R, Burt DS, Weiner HL: Nasal vaccination with a proteosome-based adjuvant and glatiramer acetate clears beta-amyloid in a mouse model of Alzheimer disease. J Clin Invest **115**: 2423-2433, 2005
14) Bard F, Cannon C, Barbour R, Burke RL, Games D, et al: Peripherally administered antibodies against amyloid beta-peptide enter the central nervous system and reduce pathology in a mouse model of Alzheimer disease. Nat Med **6**: 916-919, 2000
15) DeMattos RB, Bales KR, Cummins DJ, Dodart JC, Paul SM, et al: Peripheral anti-A beta antibody alters CNS and plasma A beta clearance and decreases brain A beta burden in a mouse model of Alzheimer's disease. Proc Natl Acad Sci U S A **98**: 8850-8855, 2001
16) Pfeifer M, Boncristiano S, Bondolfi L, Stalder A, Deller T, et al: Cerebral hemorrhage after passive anti-Abeta immunotherapy. Science **298**: 1379, 2002
17) Tang DC, DeVit M, Johnston SA: Genetic immunization is a simple method for eliciting an immune response. Nature **356**: 152-154, 1992
18) Barry MA, Lai WC, Johnston SA: Protection against mycoplasma infection using expression-library immunization, Nature **377**: 632-635, 1995
19) Ulmer JB, Donnelly JJ, Parker SE, Rhodes GH, Felgner PL, et al: Heterologous protection against influenza by injection of DNA encoding a viral protein. Science **259**: 1745-1749, 1993
20) Hoffman SL, Doolan DL, Sedegah M, Gramzinski R, Wang H, et al: Nucleic acid malaria vaccines. Current status and potential. Ann N Y Acad Sci **772**: 88-94, 1995
21) Kim HD, Maxwell JA, Kong FK, Tang DC, Fukuchi K: Induction of anti-inflammatory immune response by an adenovirus vector encoding 11 tandem repeats of Abeta1-6: toward safer and effective vaccines against Alzheimer's disease. Biochem Biophys Res Commun **336**: 84-92, 2005
22) Zhang J, Wu X, Qin C, Qi J, Ma S, et al: A novel recombinant adeno-associated virus vaccine reduces behavioral impairment and beta-amyloid plaques in a mouse model of Alzheimer's disease. Neurobiol Dis **14**: 365-379, 2003
23) Hara H, Monsonego A, Yuasa K, Adachi K, Xiao X, et al: Development of a safe oral Abeta vaccine using recombinant adeno-associated virus vector for Alzheimer's disease. J Alzheimer Dis **6**: 483-488, 2004
24) Marshall E: Gene therapy. Second child in French trial is found to have leukemia. Science **299**: 320, 2003
25) Check E: Gene therapy put on hold as third child develops cancer. Nature **433**: 561, 2005
26) Urabe M, Ding C, Kotin RM: Insect cells as a factory to produce adeno-associated virus type 2 vectors. Hum Gene Ther **13**: 1935-1943, 2002
27) Nishikawa M, Huang L: Nonviral vectors in the new millennium: delivery barriers in gene transfer. Hum Gene Ther **12**: 861-870, 2001
28) Nishikawa M, Hashida M: Nonviral approaches satisfying various requirements for effective *in vivo* gene therapy. Biol Pharm Bull **25**: 275-283, 2002

29) Ghochikyan A, Vasilevko V, Petrushina I, Movsesyan N, Babikyan D, et al: Generation and characterization of the humoral immune response to DNA immunization with a chimeric beta-amyloid-interleukin-4 minigene. Eur J Immunol **33**: 3232-3241, 2003
30) Schiltz JG, Salzer U, Mohajeri MH, Franke D, Heinrich J, et al: Antibodies from a DNA peptide vaccination decrease the amyloid burden in a mouse model of Alzheimer's disease. J Mol Med **82**: 706-714, 2004
31) Matsumoto Y, Jee Y, Sugisaki M: Successful TCR-based immunotherapy for autoimmune myocarditis with DNA vaccines after rapid identification of pathogenic TCR. J Immunol **164**: 2248-2254, 2000
32) Okura Y, Miyakoshi A, Kohyama K, Park IK, Staufenbiel M, et al: Nonviral Abeta DNA vaccine therapy against Alzheimer's disease: long-term effects and safety. Proc Natl Acad Sci U S A **103**: 9619-9624, 2006
33) Marshall E: Gene therapy death prompts review of adenovirus vector. Science **286**: 2244-2245, 1999
34) Check E: A tragic setback. Nature **420**: 116-118, 2002
35) Kay MA: AAV vectors and tumorigenicity. Nat Biotechnol **25**: 1111-1113, 2007
36) Donsante A, Miller DG, Li Y, Vogler C, Brunt EM, Russell DW, et al: AAV vector integration sites in mouse hepatocellular carcinoma. Science **317**: 477, 2007
37) Ledwith BJ, Manam S, Troilo PJ, Barnum AB, Pauley CJ, et al: Plasmid DNA vaccines: investigation of integration into host cellular DNA following intramuscular injection in mice. Intervirology **43**: 258-272, 2000
38) Bard F, Barbour R, Cannon C, Carretto R, Fox M, et al: Epitope and isotype specificities of antibodies to beta-amyloid peptide for protection against Alzheimer's disease-like neuropathology. Proc Natl Acad Sci U S A **100**: 2023-2028, 2003
39) Wilcock DM, Munireddy SK, Rosenthal A, Ugen KE, Gordon MN, et al: Microglial activation facilitates Abeta plaque removal following intracranial anti-Abeta antibody administration. Neurobiol Dis **15**: 11-20, 2004
40) Bacskai BJ, Kajdasz ST, McLellan ME, Games D, Seubert P, Schenk D, Hyman BT: Non-Fc-mediated mechanisms are involved in clearance of amyloid-beta in vivo by immunotherapy. J Neurosci **22**: 7873-7878, 2002
41) Solomon B, Koppel R, Frankel D, Hanan-Aharon E: Disaggregation of Alzheimer beta-amyloid by site-directed mAb. Proc Natl Acad Sci U S A **94**: 4109-4112, 1997
42) Dodart JC, Bales KR, Gannon KS, Greene SJ, DeMattos RB, et al: Immunization reverses memory deficits without reducing brain Abeta burden in Alzheimer's disease model. Nat Neurosci **5**: 452-457, 2002
43) DeMattos RB, Bales KR, Cummins DJ, Paul SM, Holtzman DM: Brain to plasma amyloid-beta efflux: a measure of brain amyloid burden in a mouse model of Alzheimer's disease. Science **295**: 2264-2267, 2002
44) O'Toole M, Janszen DB, Slonim DK, Reddy PS, Ellis DK, et al: Risk factors associated with beta-amyloid(1-42) immunotherapy in preimmunization gene expression patterns of blood cells. Arch Neurol **62**: 1531-1536, 2005
45) Selkoe DJ: Alzheimer's disease is a synaptic failure. Science **298**: 789-791, 2002
46) Kotilinek LA, Bacskai B, Westerman M, Kawarabayashi T, Younkin L, et al: Reversible memory loss in a mouse transgenic model of Alzheimer's disease. J Neurosci **22**: 6331-6335, 2002

J Neuropathol Exp Neurol

Vol. 67, No. 11
November 2008
pp. 1063–1071

ORIGINAL ARTICLE

Nonviral DNA Vaccination Augments Microglial Phagocytosis of β-Amyloid Deposits as a Major Clearance Pathway in an Alzheimer Disease Mouse Model

Yoshio Okura, MD, PhD, Kuniko Kohyama, MS, Il-Kwon Park, DVM, PhD, and Yoh Matsumoto, MD, PhD

Abstract

Immunotherapies markedly reduce β-amyloid (Aβ) burden and reverse behavioral impairment in mouse models of Alzheimer disease. We previously showed that new Aβ DNA vaccines reduced Aβ deposits in Alzheimer disease model mice without detectable side effects. Although they are effective, the mechanisms of Aβ reduction by the DNA vaccines remain to be elucidated. Here, we analyzed vaccinated and control Alzheimer disease model mice from 4 months to 15 months of age to assess which of several proposed mechanisms may underlie the beneficial effects of this vaccination. Immunohistochemical analysis revealed that activated microglial numbers increased significantly in the brains of vaccinated mice after DNA vaccination both around Aβ plaques and in areas remote from them. Microglia in treated mice phagocytosed Aβ debris more frequently than they did in untreated mice. Although microglia had an activated morphological phenotype, they did not produce significant amounts of tumor necrosis factor. Amyloid plaque immunoreactivity and Aβ concentrations in plasma increased slightly in vaccinated mice compared with controls at 9 but not at 15 months of age. Collectively, these data suggest that phagocytosis of Aβ deposits by microglia plays a central role in Aβ reduction after DNA vaccination.

Key Words: β-Amyloid, Alzheimer disease, DNA vaccine, Microglia.

INTRODUCTION

Alzheimer disease (AD) is the most common cause of age-related cognitive decline; it affects more than 12 million people worldwide (1). It is widely believed that accumulation of β-amyloid (Aβ) is the first event in the pathogenesis of AD and that it precedes tau phosphorylation, tangle formation, and neuron death (i.e. the amyloid cascade hypothesis) (2). Based on this hypothesis, Schenk et al (3) demonstrated that a vaccine composed of synthetic Aβ in complete Freund adjuvant induced high anti-Aβ antibody titers, leading to dramatic reductions of Aβ deposits in platelet-derived growth factor promoter–expressing amyloid precursor protein (PDAPP) transgenic mice (3). On the basis of these promising results, clinical trials with Aβ peptide (AN-1792) in conjunction with the T helper 1 adjuvant, QS-21, were initiated; however, the clinical trial was halted because some patients developed meningoencephalitis (4). Importantly, neuropathologic examination of treated patients showed apparent clearance of Aβ plaques from large areas of the neocortex (5, 6). Thus, it seems that vaccine therapy could be effective for AD if inflammatory/immune reactions are minimized.

We previously developed nonviral Aβ DNA vaccines with plasmid vectors and succeeded in reducing Aβ burden in APP23 mice without inducing side effects such as neuroinflammation (7). The mechanism of Aβ reduction after DNA vaccination, however, has not yet been elucidated. Three hypotheses explain how anti-Aβ antibodies reduce Aβ deposits in the brain (8, 9). The first is that anti-Aβ antibodies attached to Aβ plaques enhance Fc receptor–mediated phagocytosis of Aβ by microglia (10). The second mechanism is the direct effect of antibodies on Aβ, leading to the dissolution of amyloid fibrils or neutralization of Aβ oligomers (11, 12). Finally, the "peripheral sink hypothesis" postulates that anti-Aβ antibodies in the circulation results in a net efflux of Aβ from the brain into blood vessels (13, 14).

In this study, we examined whether these clearance mechanisms take place in our DNA vaccination system. We found that microglia were activated, increased in number, and phagocytosed Aβ deposits after vaccine administration. The results suggest that phagocytosis of Aβ deposits by activated microglia is a major clearance pathway of Aβ clearance after DNA vaccination and may provide important information for the development of effective new vaccines against AD.

MATERIALS AND METHODS

Animals

APP23 transgenic and wild-type B6 mice were used for analysis; and detailed information was provided in a previous

From the Department of Molecular Neuropathology, Tokyo Metropolitan Institute for Neuroscience, Fuchu, Tokyo, Japan.
Send correspondence and reprint requests to: Yoh Matsumoto, MD, PhD, Department of Molecular Neuropathology, Tokyo Metropolitan Institute for Neuroscience, 2-6 Musashidai, Fuchu, Tokyo, Japan 183-8526; E-mail: matyoh@tmin.ac.jp
This study was supported in part by Health and Labour Sciences Research Grants for Research on Psychiatric and Neurological Diseases and Mental Health and by Grants-in-Aid from the Japan Society for the Promotion of Science. Yoh Matsumoto was also supported by the Welfare and Health Fund of the Tokyo Metropolitan Government.

report (7). Plasma was obtained from mice under deep inhalation anesthesia with ethyl ether via cardiac puncture with heparinized syringes before autopsy. Anesthetized mice were then killed. All procedures of animal experimentation were approved by the ethics committee of the Tokyo Metropolitan Institute for Neuroscience and performed in accordance with institutional guidelines.

Development and Administration of DNA Vaccines

We prepared Aβ DNA vaccines using a PTarget mammalian expression system (Promega, Tokyo, Japan) and injected them into APP23 mice on a weekly and then biweekly basis as used previously (15). Two DNA vaccines were used: immunoglobulin L (IgL)–Aβ vaccine, which possesses the Igκ signal sequence of mouse immunoglobulin to improve the secretion ability, and Aβ-Fc vaccine that has the Fc portion of human immunoglobulin at the 3′ end to maintain stability. APP23 mice received DNA vaccines (100 μg in 100 μL) regularly from 4 months of age, 2 months before amyloid plaque appearance, to the termination of experiments. Mice were killed at 9 and 15 months of age.

Immunohistochemistry

Mice were killed under deep anesthesia, and the brains were removed and immersion fixed in 4% paraformaldehyde. Paraffin-embedded sections were stained with monoclonal antibodies (mAbs) 6F/3D against Aβ8-17 (DAKO, Tokyo, Japan) and Iba-1 for microglia (WAKO, Tokyo, Japan). Sections were pretreated in formic acid for 3 minutes for 6F/3D staining and 0.1% trypsin for 10 minutes at 37°C for Iba-1 staining. After pretreatment, the sections were incubated in the primary mAbs followed by biotinylated horse anti-mouse immunoglobulin G (IgG) and horseradish peroxidase (HRP)–labeled Vectastain Elite ABC kit (Vector, Funakoshi, Tokyo, Japan). Horseradish peroxidase–binding sites were detected in 0.005% diaminobenzidine and 0.01% hydrogen peroxide. For confocal microscopic analysis, fluorescein isothiocyanate anti-mouse IgG and Cy-3 anti-rabbit IgG were used as secondary antibodies for 6F/3D and Iba-1 staining, respectively. The presence or absence of IgG depositions on Aβ plaques was determined by incubation of sections with biotinylated horse anti-mouse IgG followed by HRP-labeled Vectastain Elite ABC kit.

Quantitative Analysis of Aβ Burden and Microglia

β-Amyloid deposits were quantitated in the cerebral cortex and hippocampus according to the method used previously (15). All the procedures were performed by an individual blinded to the experimental conditions. The amyloid load was measured in 10 fields from the cingulate to retrosplenial cortex in the left hemisphere per mouse. Each field measured 600 × 400 μm and was randomly chosen. Analysis of the entire hippocampus was performed in a similar manner. β-Amyloid deposits that occupied the field were expressed as pixels using National Institutes of Health (NIH) image software.

After Iba-1 staining, the densities of microglia were determined by counting them in randomly selected 10 fields (600 × 400 μm each) from the cingulate to retrosplenial cortex in the left hemisphere of mice (n = 4–6 in each group). Microglia around the plaque (periplaque area) and those remote from the plaque (remote area) were counted separately and expressed as the mean ± SE per field. Using double-stained sections for Aβ and microglia, the densities of phagocytosing microglia were determined in a similar manner under confocal microscopy.

Western Blotting

Brain tissues were homogenized and sonicated in 10 volumes of Tris-buffered saline buffer in the presence of protease inhibitors. One milliliter of formic acid was added to 300 μg of homogenate in 10 μL. After a brief incubation, formic acid was vacuum dried with an acid-proof vacuum evaporator (miVac DNA, Scrum, Tokyo, Japan). After adding NuPAGE LDS sample buffer (Invitrogen, Tokyo, Japan), the samples were incubated at 70°C for 10 minutes and were run on NuPAGE 12% Bis-Tris gel (Invitrogen) (16). Before electrophoresis, protein concentration of each sample was determined, and the volume for loading was adjusted (equivalent to 40 μg); samples were then transferred to polyvinylidene difluoride membrane (Immobilon-P; Millipore, Tokyo, Japan). After blocking with 10% nonfat milk, the blots were incubated with anti-human Aβ 1–17 antibody (6E10; Cambridge, United Kingdom; 1:100) at 4°C overnight followed by incubation with Trueblot HRP-conjugated anti-mouse IgG (eBioscience, San Diego, CA; 1:1000) for 1 hour. The blots were developed by enhanced chemiluminescence reagents (Immunostar Kit Wako; WAKO) according to the manufacturer's instructions. The density of each band obtained by Western blot analysis was measured with a scanning laser densitometer (GS-700, Bio-Rad, Hercules, CA) and analyzed using the NIH image software.

Real-time Polymerase Chain Reaction

Total RNA was extracted from the indicated tissues using an RNAqueous Kit (Ambion), and complementary DNA was then synthesized by reverse transcription using a High Capacity cDNA Reverse Transcription Kit (Applied Biosystems, Foster City, CA). SYBR Green real-time polymerase chain reactions (PCRs) were performed on an ABI PRISM 7500 sequence detection system (Applied Biosystems) in a total volume of 25 μL using the SYBR Premix Ex Taq (Takara Bio, Otsu, Japan). Each PCR was performed in duplicate using thermocycler conditions: Stage 1, 95°C for 10 minutes for 1 cycle and Stage 2, 95°C for 15 seconds and 58°C for 1 minute for 50 cycles. All primers were designed on an intron-exon junction to prevent coamplification of genomic DNA, and their sequences were shown in previous reports (17, 18). Relative quantification of messenger RNA (mRNA) was performed using the standard curve method. Glyceraldehyde-3-phosphate dehydrogenase was used as internal control. The absence of nonspecific amplification was confirmed by dissociation curve analysis.

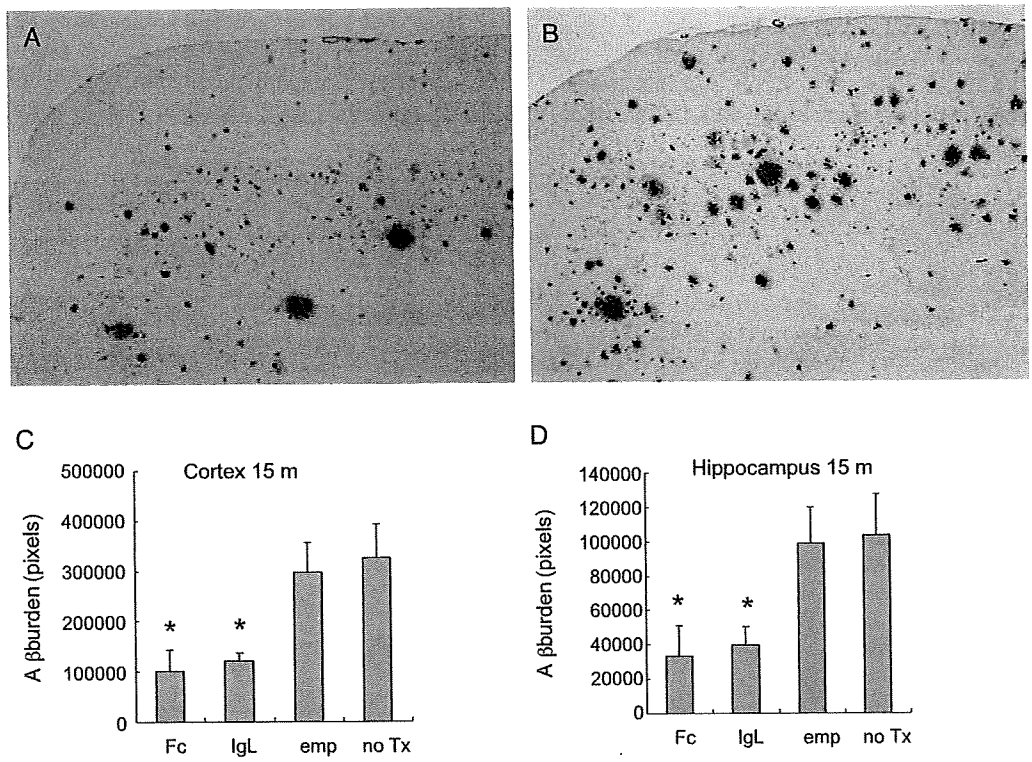

FIGURE 1. β-Amyloid (Aβ) reduction after DNA vaccination in mice at 15 months of age. There were fewer Aβ deposits in the frontal cortex of a mouse that had been treated with the Aβ-Fc vaccine **(A)** than in frontal cortex of a control mouse **(B)**. Semiquantitative analysis revealed that Aβ deposits were significantly reduced (* = $p < 0.01$) in the cortex of vaccinated mice (30.6% of untreated mice) **(C)**. β-Amyloid deposits in the hippocampus were also significantly reduced (* = $p < 0.01$) after vaccine treatment **(D)**. emp, empty vector; no Tx, untreated.

Tissue Amyloid Plaque Immunoreactivity Assay

Plasma to be tested were diluted to ×100, ×300, ×1,000, and ×3,000, and then applied to formic acid-pretreated APP23 brain sections, followed by incubation with biotinylated horse anti-mouse IgG and HRP-labeled Vectastain Elite ABC kit (Vector). The maximal dilution of plasma that gave positive staining was estimated as the amyloid plaque immunoreactivity titer.

Quantification of Tumor Necrosis Factor in the CNS Tissues and Plasma Aβ With ELISA

Brain tissue was homogenized in lysis buffer, and the supernatant was harvested after centrifugation. Each sample was adjusted to 10 mg/mL. The levels of brain tumor necrosis factor (TNF) and plasma Aβ were determined using the Mouse TNF Instant ELISA (Bender MedSystems, Vienna, Austria) and human Aβ (1–42) ELISA Kit (WAKO),

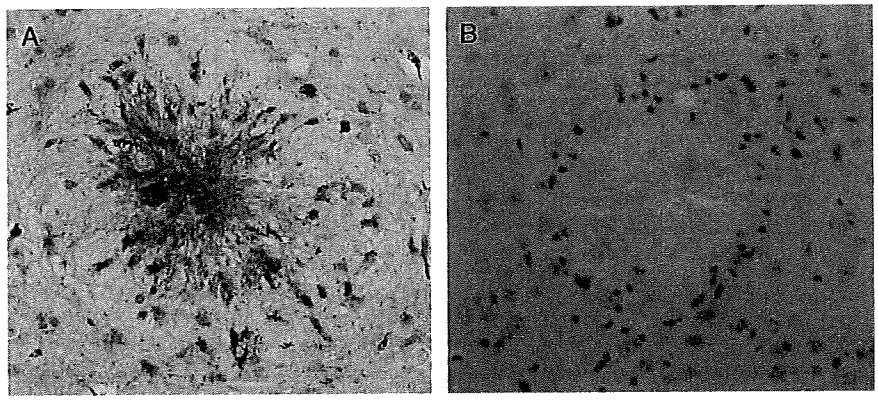

FIGURE 2. Immunoglobulin G (IgG) in the brains of DNA vaccine–treated and untreated APP23 mice at age 15 months. β-Amyloid (Aβ) plaques in the brain of an Aβ-Fc vaccine–treated mouse stained positively for IgG **(A)**, whereas a plaque in an untreated mouse was completely negative **(B)**. Immunohistochemistry with anti-mouse IgG. Original magnification: 200×.